Large-Scale Optical Phased Array Based on a Multi-Layer Silicon-Nitride-on-Silicon Photonic Platform

Liangjun Lu[1, 2, *], Weihan Xu[1], Yuyao Guo[1, 2], Chuxin Liu[1], Jianping Chen[1, 2], Linjie Zhou[1, 2]
[1]*State Key Laboratory of Advanced Optical Communication Systems and Networks, Shanghai Key Lab of Navigation and Location Services, Shanghai Institute for Advanced Communication and Data Science, Department of Electronic Engineering, Shanghai Jiao Tong University, Shanghai 200240, China*
[2]*SJTU-Pinghu Institute of Intelligent Optoelectronics, Pinghu 314200, China*
* luliangjun@sjtu.edu.cn

Abstract: We review our recent progress on a chip-scale LiDAR transmitter on a multi-layer Si_3N_4-on-Si photonic platform. Experimental results show the high optical power budget of the chip and the feasibility for FMCW ranging.

1. Introduction

Solid-state LiDAR based on optical phased array (OPA) can realize lens-free beam-forming and inertial-free beam-steering for reliable and software-defined 3D imaging [1, 2]. For various applications, including autonomous driving, smart logistics and intelligent infrastructure, chip-scale LiDARs with long-range operation and high-resolution detection are in high demand. Therefore, many works focus on increasing the input optical power to the OPAs and implementing a larger emitting aperture for a higher angular solution. Recently, the silicon nitride (Si_3N_4) on silicon (Si) platform [3, 4], which combines the low linear and nonlinear loss of Si_3N_4 waveguides with high tuning efficiency of Si waveguides, has been used for high-performance OPAs for its high optical power budget and ease of mass integration. Besides, it is highly desired to integrate a high-power laser source with the OPA. Coherent light detection based on the frequency-modulated continuous wave (FMCW) scheme is very suitable for OPA-based LiDARs. Typically, the detection resolution is affected by the frequency chirp's linearity, and the laser's dynamic coherence determines the detection range. For the grating-based 2D-OPAs, the elevation steering angle also depends on the wavelength tuning range. Therefore, integrated external cavity lasers (ECLs), which possess a wide wavelength tuning range and a narrow linewidth, are essential for LiDAR-oriented OPAs.

This paper reviews our recent progress on a fully integrated solid-state LiDAR transmitter fabricated on the multi-layer Si_3N_4-on-SOI platform. It comprises a III/V-Si_3N_4 hybrid integrated external cavity laser (ECL) and a 256-channel OPA. We experimentally verify the high optical power budget of our chip and the feasibility for FMCW ranging.

2. Device structure and packaging

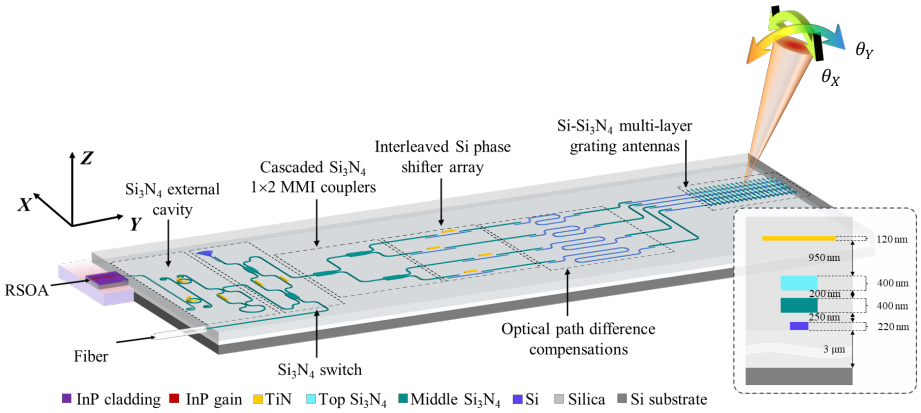

Fig. 1. Schematic structure of the LiDAR transmitter on the multi-layer Si_3N_4 on SOI platform.

Figure 1 shows the LiDAR transmitter chip, which consists of a III/V-Si_3N_4 hybrid integrated ECL for narrow-linewidth wide-tunable laser source and a 256-channel optical phased array. A Si_3N_4 Mach–Zehnder interferometer (MZI) switch is inserted between the ECL and the OPA so that we can also choose an off-chip laser source coupled through the fiber. The OPA is composed of eight stages of cascaded Si_3N_4 1×2 multimode interferometers (MMIs) power splitters, 256 interleaved silicon thermo-optic (TO) phase shifters for efficient element-wise phase control

with suppressed thermal crosstalk, silicon delay lines for optical path differences (OPDs) compensation between the channels, and Si-Si_3N_4 multi-layer grating aperture for highly directional beam-forming and steering. For the hybrid-integrated ECL, a reflective semiconductor optical amplifier (RSOA) is butt-coupled with a Si_3N_4 wavelength-selective reflector based on two Vernier micro-ring resonators, and a tunable Sagnac loop reflector (TSL). The InP waveguide on the front side is slanted by 8° and anti-reflection (AR) coated to reduce reflectivity. The detail of the device design can be seen in [5]. Figure 2 shows the packaging process and the packaged chip. The RSOA was first loaded onto a customized submount via eutectic bonding [1]. The COC (chip on carrier) was then actively aligned with the spot-size converter of the ECL on the transmitter chip. The sub-assembly was further loaded on a raised platform with a heatsink to facilitate thermal dissipation and wire-bonding. Finally, a fiber array (FA) was attached for calibration of the ECL as well as the OPA. Note that another RSOA submount was used as a makeshift interposer in Fig. 2(b) to shorten the wire bond between the RSOA and the PCB for improved robustness.

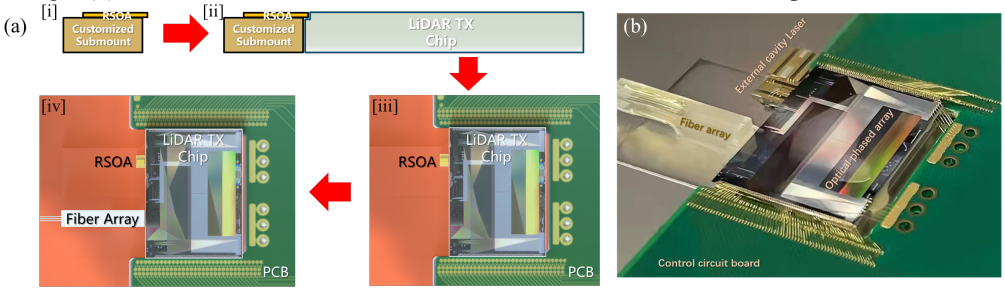

Fig. 2. (a) [i-iv] Packaging process of the device, individual wire bonds are omitted; (b) Picture of the packaged chip.

3. Experimental results

We have reported the test results of both the ECL and the OPA in [6]. The ECL has a wide wavelength tuning range of 100 nm and a narrow intrinsic linewidth of 2.8 kHz, while the OPA exhibits a wide field-of-view of 50° × 16° with a full width at half maximum beam divergence of 0.051° × 0.016° in broadside direction. Here, we further validated the chip's power budget. For high-power handling of the bus Si_3N_4 waveguide, a high-power continuous-wave laser of up to 2 watts was launched into the U-bend reference ports of the chip via the FA. As shown in Fig. 3(a), the coupling loss is about 3.06 dB/facet, meaning the injected power is about 1 watt. By increasing the power gradually while monitoring the output power with a power meter, the throughput shows high linearity, indicating negligible nonlinear loss, as shown in Fig. 3(b). Additionally, by placing a photodiode above the aperture at different distances, the beam-forming loss is determined to be about 17 dB. The larger beam-forming loss and larger loss at a longer distance are attributed to the inconsistency between the grating antennas and the phase noise within each antenna. These factors lead to a significantly higher noise floor and lower beam-forming efficiency, prohibiting LiDAR demonstration with the on-chip ECL.

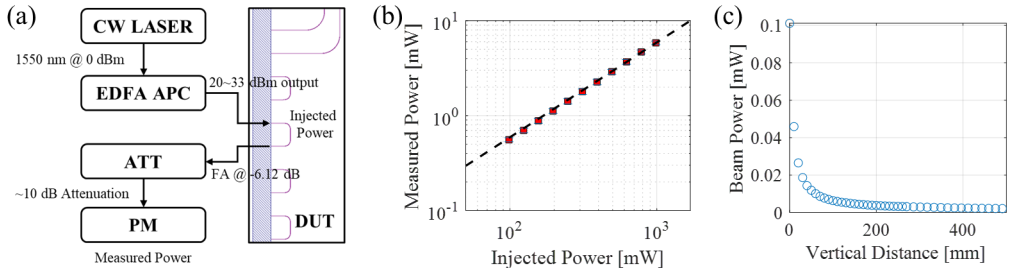

Fig. 3. (a) Experiment setup for power handling validation; (b) Throughput of the reference port with high injected power; (c) Measured beam power with a photodiode along the propagation direction of the beam.

Nevertheless, we provided preliminary results to demonstrate the feasibility of the fully integrated LiDAR transmitter. Figure 4 shows the experimental setup. To begin with, the driving signal of the onboard ECL was pre-distorted according to our previous work [7] and applied with an arbitrary waveform generator. The generated FMCW signal has a chirp bandwidth of 0.9 GHz, a repetition rate of 1 kHz and a linearity of 99.74%. About 90% of the output power was launched into the OPA, while 10% was coupled off-chip via the FA as the reference light. The majority of the optical power was then selected by the Si_3N_4 optical switch and left the chip via the emitting aperture of grating antennas. A collimator collected the emitted beam at a distance of 0.5 m to represent the received laser echo. Delay fibers of different lengths were introduced on the reference path to emulate targets at different distances.

The light in the echo and reference paths interfered in a 50:50 fiber coupler and was subsequently detected by a balanced photodetector. The temporal beat signal was recorded by an oscilloscope and converted into the beat signal spectrum via the Fast-Fourier transform.

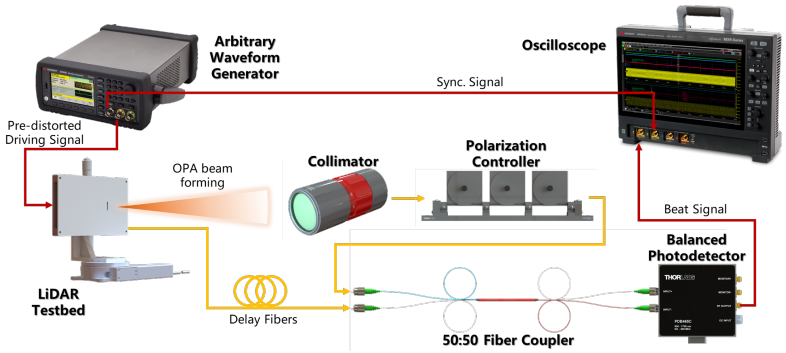

Fig. 4. Experiment setup for the emulated FMCW ranging

Figure 5 (a) presents the beat signal spectra at different delay fiber lengths, and Fig. 5(b) shows the extracted peak frequencies of the beat signals against the extended fiber lengths. The linear regression of the latter relationship enjoys a high determination coefficient of 99.7% up to a range of 50 meters. This indicates that the onboard laser supports FMCW ranging, and the implementation of the OPA beam-former in the same chip introduces no penalty to the system.

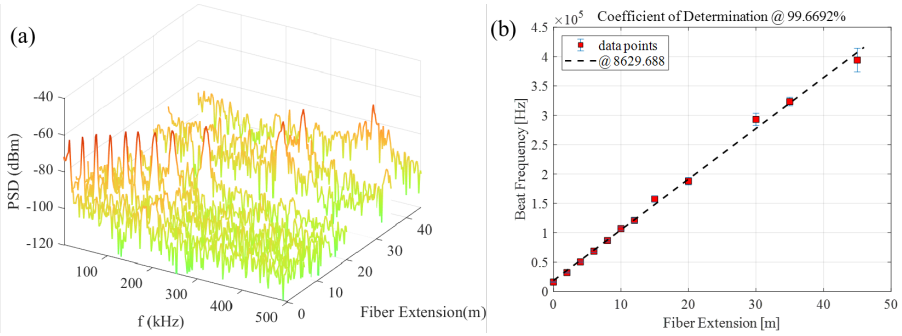

Fig. 5. (a) Beat signal spectra with different delay fiber lengths; (b) Linear regression of the peak frequencies of the beat signals vs the extended fiber lengths.

4. Conclusion

We report the ranging characteristics of our LiDAR transmitter based on the multi-layered Si_3N_4-on-Si platform. By synchronous modulation of both the phase shifter and the Vernier rings, we can further increase the chirp bandwidth to ~ 8 GHz [8]. Besides, an analogue electro-optical phase-locked loop can improve its range resolution for a longer target range at 200 m [9]. These preliminary results validate the feasibility of our approach for co-integration of the laser and the beam scanner in a single chip.

1. N. Li, C. P. Ho, J. Xue, L. W. Lim, G. Chen, Y. H. Fu, and L. Y. T. Lee, "A Progress Review on Solid- State LiDAR and Nanophotonics-Based LiDAR Sensors," Laser & Photonics Reviews **16**, 2100511 (2022).
2. S. Zhao, J. Chen, and Y. Shi, "All-Solid-State Beam Steering via Integrated Optical Phased Array Technology," Micromachines **13**, p.894 (2022).
3. W. D. Sacher, Y. Huang, G.-Q. Lo, and J. K. Poon, "Multi-layer silicon nitride-on-silicon integrated photonic platforms and devices," Journal of Lightwave Technology **33**, 901-910 (2015).
4. W. D. Sacher, J. C. Mikkelsen, P. Dumais, J. Jiang, D. Goodwill, X. Luo, Y. Huang, Y. Yang, A. Bois, and P. G.-Q. Lo, "Tri-layer silicon nitride-on-silicon photonic platform for ultra-low-loss crossings and interlayer transitions," Optics express **25**, 30862-30875 (2017).
5. W. Xu, Y. Guo, X. Li, C. Liu, L. Lu, J. Chen, and L. Zhou, "Fully Integrated Solid-State LiDAR Transmitter on a Multi-Layer Silicon-Nitride-on-Silicon Photonic Platform," Journal of Lightwave Technology **41**, 832-840 (2023).
6. W. Xu, Y. Guo, X. Li, C. Liu, L. Lu, J. Chen, and L. Zhou, "Fully Integrated Solid-State LiDAR Transmitter on a Multi-Layer Silicon-Nitride-on-Silicon Photonic Platform," in *Optical Fiber Communication Conference (OFC) 2022*, Technical Digest Series (Optica Publishing Group, 2022), Th1E. 4.
7. C. Liu, Y. Guo, W. Xu, L. Lu, J. Chen, and L. Zhou, "Improving the frequency chirp linearity of a frequency-modulated continuous-wave laser," in *26th Optoelectronics and Communications Conference*, OSA Technical Digest (Optical Society of America, 2021), T4E.7.
8. C. Liu, L. Lu, Y. Guo, X. Li, J. Chen, and L. Zhou, "Hybrid integrated frequency-modulated continuous-wave laser with synchromous tuning," Journal of Lightwave Technology 40, 5636-5645 (2022).
9. C. Liu, R. Xu, W. Xu, L. Lu, Y. Guo, Y. Li, J. Chen, and L. Zhou, "High-precision FMCW ranging with a hybrid-integrated external cavity laser," in *Opto-Electronics and Commnunications Conference (OECC)* 2023, IEEE, 23580195.